SCIENCE CHINA Chemistry

Tetra-EDOT substituted 3D electrochromic polymers with lower band gaps

Shi Jingjing, Murtaza Imran, Shao Shan, Zhu Xiaosi, Zhao Yang, Zhu Mengmeng, Goto Osamu and Meng Hong

Citation: SCIENCE CHINA Chemistry **60**, 90 (2017); doi: 10.1007/s11426-016-0303-0

View online: http://engine.scichina.com/doi/10.1007/s11426-016-0303-0

View Table of Contents:http://engine.scichina.com/publisher/scp/journal/SCC/60/1

Published by the Science China Press

SCIENCE CHINA Chemistry

SCIENCE CHINA
Chemistry

• ARTICLES •
· SPECIAL TOPIC · Electrochromics

January 2017 Vol.60 No.1: 90–98
doi: 10.1007/s11426-016-0303-0

Tetra-EDOT substituted 3D electrochromic polymers with lower band gaps

Jingjing Shi[1], Imran Murtaza[2,3], Shan Shao[1], Xiaosi Zhu[1], Yang Zhao[2], Mengmeng Zhu[1], Osamu Goto[1] & Hong Meng[1,2*]

[1]*School of Advanced Materials, Peking University Shenzhen Graduate School, Shenzhen 518055, China*
[2]*Key Laboratory of Flexible Electronics & Institute of Advanced Materials, Jiangsu National Synergetic Innovation Center for Advanced Materials, Nanjing Tech University, Nanjing 211816, China*
[3]*Department of Physics, International Islamic University, Islamabad 44000, Pakistan*

Received July 26, 2016; accepted September 27, 2016; published online December 7, 2016

A couple of novel electrochromic materials poly(2,3,4,5-tetrakis(2,3-hydrothieno[3,4-*b*]dixin-5-yl)-1-methyl-1*H*-pyrrole) (P(*t*-EDOT-mPy)) and poly(5,5′,5″,5‴-(thiophene-2,3,4,5-tetrayl)tetrakis(2,3-dihydrothieno[3,4-*b*][1,4]dioxine)) (P(*t*-EDOT-Th)) are electrodeposited via multi-position polymerization of their *tetra*-EDOT substituted monomers *t*-EDOT-mPy and *t*-EDOT-Th, respectively. Compared with the linear 2D structured poly(thiophene) (E_g=2.2 eV) and poly(2,5-bis(2,3-dihydrothieno[3,4-*b*][1,4]dioxin-5-yl)thiophene) (E_g=1.7 eV), P(*t*-EDOT-Th) (E_g=1.62 eV) has the lowest band gap. Hence, we speculate that the band gaps of the two polymers, having 3D structures, are decreased in contrast to non-substituted polymers or *bi*-EDOT substituted polymers, thiophene and 1-methyl-1*H*-pyrrole. The results indicated that P(*t*-EDOT-Th) thin films are more stable and show higher transmittance amid two polymers, which may find their utilization in organic optoelectronics.

conjugated 3D polymers, electrochromic, polythiophene, polypyrrole, EDOT, low band gap, electrochemistry

Citation: Shi J, Murtaza I, Shao S, Zhu X, Zhao Y, Zhu M, Goto O, Meng H. *Tetra*-EDOT substituted 3D electrochromic polymers with lower band gaps. *Sci China Chem*, 2017, 60: 90–98, doi: 10.1007/s11426-016-0303-0

1 Introduction

Electrochromic materials have the property of change or bleaching of color as a result of an electron-transfer (redox) process or by applying a sufficient electrochemical potential [1]. They have been broadly applied in displays [2], smart windows [3], anti-glare rear-view mirrors [4], camouflage technologies [5] and supercapacitors [6] due to the advantages of low applied potential, reversible color exchange, reasonable optical memory, short response time, near infrared absorption, high coloration efficiency, long life-time cycle, low cost, high flexibility, large-scale processability and tunable chemical structures [7,8]. For example, electrochromic materials have been applied in the Alteos interactive window system of Boeing 787 Dreamliner [9]. It not only controls the light absorption based on the color exchanges, but also intensely attracts the passengers' interest giving them an innovative experience.

As widely investigated conducting polymers, poly(thiophene)s (PTs) and poly(pyrrole)s (PPys) have revealed comprehensive research in organic electrochromic devices (OECDs), organic field effect transistors (OTFTs), organic photovoltaics (OPVs), organic light-emitting diodes (OLEDs) and radiofrequency identification (RFID) tags. Both of them are plausible candidates for electrochromic devices on account of their stability, color tuning and relatively easier electrochemical synthesis [1,10,11]. In addition, poly(3,4-ethylenedioxythiophene) (PEDOT) [1,10,12] as

*Corresponding author (email: menghong@pkusz.edu.cn)

is well known, having the ability to change color, has attracted extensive attention over the past several decades [13]. PEDOT has an intense non-covalent intramolecular S–O interaction with circumambient EDOT groups because of their donor effect.

Among all the conjugated polymers reported so far, band gap is one of the most imperative parameters in evaluating their electrochromic performance [10]. Thus, in order to indirectly achieve the desirable electrochromic properties, band gap can be regulated to adjust the visible light absorption in polymers. The intramolecular interactions between the high band gap materials PT (E_g=2.2 eV) and PPy (E_g=2.7 eV), and low band gap material PEDOT (E_g=1.6 eV), will result in a lower band gap and a unique combination of stability [14]. Thus, we envisioned that these polymer groups of PTs, PPys and PEDOT (molecular structure shown in Figure 1) [10] can be combined to better tune the electroactive properties such as band gap.

Patra *et al.* [15] synthesized the two-dimensional (2D) material poly(BEDOT-T), with band gap between PPy and PEDOT [16], until now, a large number of multi-position materials have been synthesized by electropolymerization, for instance, the core of benzene, truxene, 2,4,6-tri(2′-thienyl)-1,3,5-triazine [17] and triphenylamine-based [18] star-shaped materials were synthesized with *tetra*-positions. Most of the *tetra*-position materials have three-dimensional (3D) [19] structure and superior electrochromic properties, such as *tetra*-EDOT substituted bithiophene, 2,3,4,5-tetrathiophenyl-thiophene, 1,3,5-tristhienyl-benzene [20] and diphenylphosphine (DPP) [21,22].

In our previous work, we have synthesized a series of *tetra*-EDOT substituted core compounds and obtained different polymers at different potentials because of having a variety of substitution sites [16]. Serendipitously, the materials which are *tetra*-EDOT substituted have 3D structures [23], clear color changes and exceptional properties.

Herein, we propose multi-substituted EDOT units on the thiophene and pyrrole cores by designing and synthesizing two novel materials (2,3,4,5-tetrakis (2,3-dihydrothieno[3,4-*b*][1,4]dioxin-5-yl)-1-methyl-1*H*-pyrrole (*t*-EDOT-mPy) and 5,5′,5″,5‴-(thiophene-2,3,4,5-tetrayl) tetrakis(2,3-dihydrothieno[3,4-*b*][1,4]dioxine) (*t*-EDOT-Th)) (Scheme 1). In our study, both the two polymer materials have lower band gaps as compared to their non-substituted polymers.

Since the properties of two polymer materials are similar to PEDOT, we can speculate that both the materials can replace PEDOT to some extent. The polymers have lower lowest unoccupied molecular orbital (LUMO) and appropriate band gap, and can be applied as hole injection materials. We believe that these kinds of materials can have a wide range of applications in the field of organic electronics.

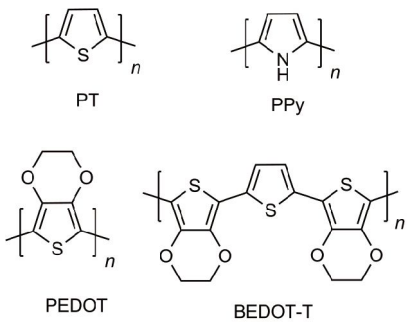

Figure 1 Molecular structures of the polymers reported in literature [10].

2 Experimental

2.1 Materials

All the chemicals were purchased from Energy Chemical (China), the chemical reagents like toluene, dichloromethane (DCM), tetrahydrofuran (THF), acetonitrile (ACN) were dried and distilled over calcium hydride under nitrogen. Palladium catalyst was purchased from TCI (Japan). $LiClO_4$, propylene carbonate (PC), poly(methyl metacrylate) (PMMA) (M_W=1300000), tetrabutylammonium hexafluorophosphate ($TBAPF_6$) were purchased from Aldrich (USA) and were used without further purification. The 2,3,4,5-tetrabromo-1-methyl-1*H*-pyrrole, perbromothiophene and tributyl(2,3-dihydrothieno[3,4-*b*][1,4]dioxin-5-yl)stannane were synthesized according to a previously reported procedure [24,25].

2.2 Equipment

The monomers were analyzed by nuclear magnetic resonance spectroscopy (NMR), mass spectra (MS) used by Shimadzu LCMS2020 (Japan) and ABI Qstar Elite (USA). Ultraviolet-visible-near infrared (UV-Vis-NIR) spectrum was recorded on a PerkinElmer Lambda 750 spectrophotometer (USA). All electrochemical studies were carried out using a CHI620E electrochemical workstation. Bruker Multimode8 atomic force microscope (AFM; Germany) was used to make morphological studies.

2.3 Electropolymerization and electrochemical tests

All the electrochemical tests and electropolymerization of the

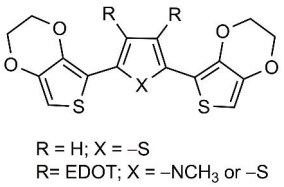

Scheme 1 Molecular structures of the monomers.

monomers were performed in a three electrode cell containing indium tin oxide (ITO) coated glass or Pt (d=0.2 cm) as the working electrode, Pt as the counter electrode and a Ag wire as the pseudo reference electrode, using CHI620E electrochemical workstation. Both the monomers were deposited by oxidative electropolymerization in 0.1 M $TBAPF_6$ (supporting electrolyte) and THF solution.

3 Results and discussion

3.1 Synthesis procedure of monomer

3.1.1 2,3,4,5-Tetrakis(2,3-dihydrothieno[3,4-*b*][1,4]dioxin-5-yl)-1-methyl-1*H*-pyrrole (*t*-EDOT-mPy)

The monomer *t*-EDOT-mPy was synthesized by Stille coupling and the synthetic strategy of the target compound is shown in Scheme 2. Compound 2,3,4,5-tetrabromo-1-methyl-1*H*-pyrrole (2 g, 5.1 mmol) and compound tributyl(2,3-dihydrothieno[3,4-*b*][1,4] dioxin-5-yl)stannane (11 g, 25 mmol) was dissolved in anhydrous toluene (200 mL). $Pd(PPh_3)_4$ (0.47 g, 0.408 mmol, 8%) was added and stirred after purged with argon for 30 min. The mixture was then stirred at 120 °C in pressure flask for 15 h before cooling it down to room temperature. The reaction mixture was washed with DCM, H_2O and brine. After drying with anhydrous magnesium sulfate, solvent was removed by rotary evaporation. The crude product was purified by silica gel chromatography (PE:DCM=1:1, 1:2, 1:4, 1:6) to finally obtain *t*-EDOT-mPy monomer (orange powder, 1.1 g, yield 33.6%). EI, MS *m*/*z* (%) 642 (M^+) ^{1}H NMR (300 MHz, $CDCl_3$, ppm) δ 6.69 (d, J=5.1 Hz, 4H), 4.13 (dd, J=5.2, 2.5 Hz, 8H), 4.04 (dd, J=5.1, 2.6 Hz, 8H), 3.36 (s, 3H) (Scheme 2).

3.1.2 5,5′,5″,5‴-(thiophene-2,3,4,5-tetrayl)tetrakis(2,3-dihydrothieno[3,4-*b*][1,4]dioxine) (*t*-EDOT-Th)

The synthetic procedure of *t*-EDOT-Th is similar to the process of t-EDOT-mPy. Finally, pure *t*-EDOT-Th monomer was obtained in the form of yellow powder with isolated yield 53.2%. EI, MS *m*/*z* (%) 645 (M^+) (^{1}H NMR (300 MHz, $CDCl_3$, ppm) δ 6.44 (s, 4H), 4.35 (td, J=3.6, 2.2 Hz, 8H), 4.26 (td, J=3.5, 2.1 Hz, 8H) (Scheme 2).

The precusor of *t*-EDOT-mPy was metamorphic after being placed in vacuum drying oven for 2 weeks under room temperature, because of solid-state polymerization [26]. Also the highest occupied molecular orbital (HOMO) and LUMO levels were measured using density functional theory at the B3LYP/6-31G* level. The HOMO level of *t*-EDOT-mPy is –4.91 eV and the LUMO level is –0.36 eV (for *t*-EDOT-Th, the HOMO level is –5.00 eV and the LUMO level is –1.13 eV). The LUMO of *t*-EDOT-mPy is so high that it easily degrades and this conclusion is verified by the experimental results.

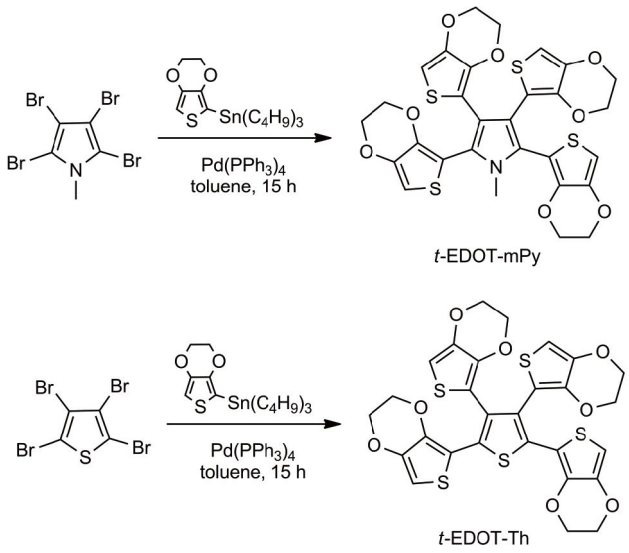

Scheme 2 Synthesis procedures of *t*-EDOT-mPy and *t*-EDOT-Th *via* Stille coupling.

3.2 Mechanism of electropolymerization (anion-participated cation radical polymerization)

The polymerization of the monomers was performed by cyclic voltammetry and the mechanism of electropolymerization was anion-participated cation radical [27]. Firstly, the monomers were adsorbed on the surface of the substrate. Secondly, each monomer lost an electron to form radical cation under oxidation potential and anions combined with radical cations to reduce the electrostatic repulsion [28]. Thirdly, two radicals were coupled, generating dihydro dimer dication, which lost the two protons to form a dimer. The dimers lost electrons further and coupled under the applied potential. With the gradual increase in the polymerization degree, the insoluble polymer accumulated on the substrate regularly. Different conditions (solvents, scan rate etc.) correspond to different morphologies, which is ascribed to different initial arrangements of oligomers [4,29,30]. Therefore, we have to choose optimal experimental conditions. During the process of electropolymerization, the step that two radicals coupled and lost protons is rate-limiting step [31,32].

3.3 Electrochemical properties

The oxidative polymerization was implemented by three electrode cell in THF solution containing 7.8×10^{-4} M monomer (*t*-EDOT-mPy) or 7.8×10^{-3} M monomer (*t*-EDOT-Th). Figure 2(a) shows the polymerization process of *t*-EDOT-mPy and a reversible redox process quickly grown between 0 and 1.2 V at a scan rate of 100 mV s^{-1}. The first cycle of electropolymerization demonstrated irreversible monomer oxidation peaks. P(*t*-EDOT-Th) was electrodeposited between –0.8 and 1.3 V at a scan rate of

100 mV s^{-1} [33]. At last, the thin films of P(*t*-EDOT-mPy) and P(*t*-EDOT-Th) with thickness of 223 and 267 nm respectively were obtained.

Herein, it is critical to ensure the position of electropolymerization since both the polymers have multi positions. Based on ^{1}H NMR giving the chemical shift and computational simulation revealing distribution of electron density, we assumed that four positions are similar, that is to say, the oxidation potentials of four positions are nearly the same. All the four positions could electropolymerize together under a reasonable potential. Due to the existence of four EDOT groups, there are three different connections between radical cations and the EDOT units are connected through the α-α, β-β, α-β positions of pyrrole and thiophene core. It is known that the α-β conjugation would introduce steric hindrance comparing with α-α and β-β connections [16,34]. Consequently, both α-α and β-β connections result in 3D structures. Insets in Figure 2 give the electropolymerization mechanism of the two materials.

As an important property of the electrochromic polymers, the scan rate dependence of the two polymeric films were investigated by cyclic voltammetry (CV) in the same system within a scan rate range of 50 to 300 mV s^{-1}. As shown in Figure 3(c, d), the peak current intensities of both polymers have a good linear dependence on the scan rate, indicating that both redox processes are non-diffusion limited and the electroactive polymer films are well-adhered to the Pt electrode.

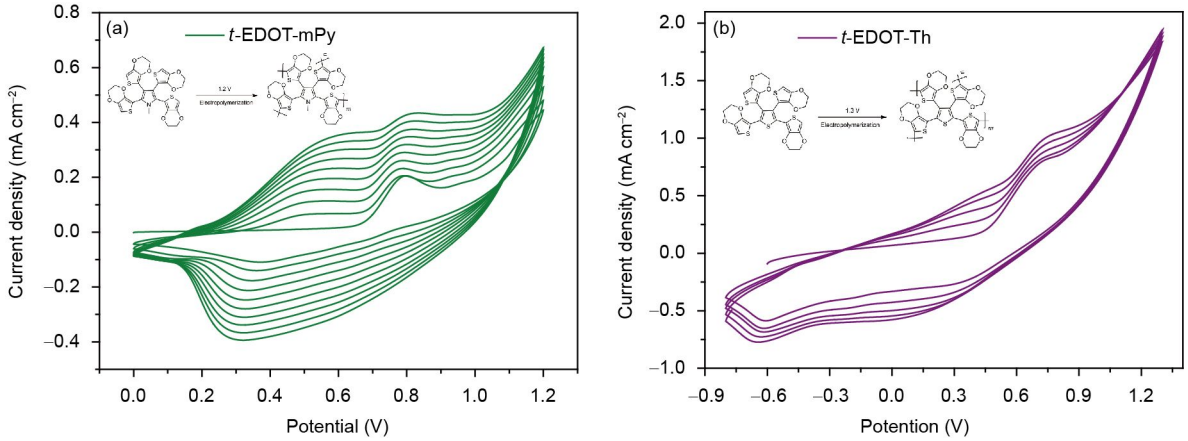

Figure 2 Electrochemical polymerization process of (a) *t*-EDOT-mPy and (b) *t*-EDOT-Th on Pt disk electrode (d=0.2 cm) (color online).

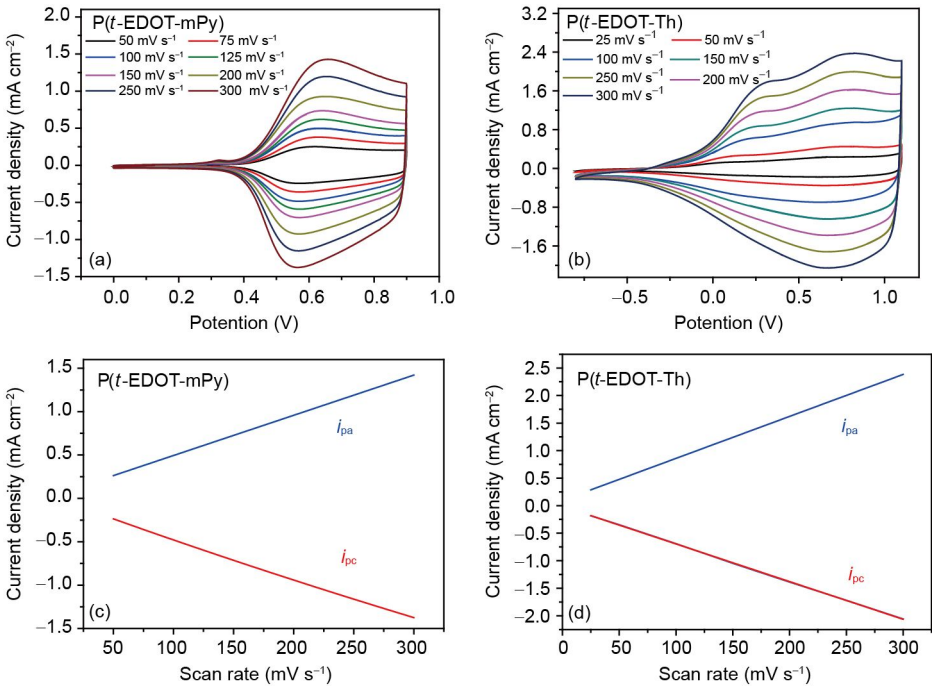

Figure 3 Cyclic voltammetry of (a) P(*t*-EDOT-mPy) and (b) P(*t*-EDOT-Th) at scan rates of 50, 75, 100, 150, 200, 250 and 300 mV s^{-1}; linear relationships of (c) P(*t*-EDOT-mPy) and (d) P(*t*-EDOT-Th) between peak current densities and scan rates (color online).

Figure 4 shows the single cyclic voltammograms of both polymer films. P(*t*-EDOT-mPy) presents very well-defined single redox processes. Initially, the polymer loses one electron, followed by the loss of two or more electrons until totally doped and the polymer films form polarons and bipolarons as charge carriers during the process [31].

Tetra-EDOT substituted thiophene and 1-methyl-1*H*-pyrrole displayed lower onset oxidation potentials in comparison with P(1-methyl-1*H*-pyrrole) [32]. The oxidation onset potential of P(*t*-EDOT-mPy) is 0.33 V. The P(*t*-EDOT-mPy) polymer has the anodic peak potential at 0.61 V and cathodic peak potential at 0.56 V with a scan rate of 100 mV s^{-1}. The value of HOMO is calculated as –4.59 eV (the potential was calibrated to the ferrocene redox couple $E°(Fc/Fc^{+})=0.54$ V (Ag wire)). The oxidation onset potential of P(*t*-EDOT-Th) is –0.1 V and the calculated value of HOMO is –4.16 eV. Unlike P(*t*-EDOT-mPy) films, P(*t*-EDOT-Th) has two anodic peak potentials at 0.18 and 0.72 V and one broad cathodic peak at 0.70 V under the same condition and the potential of P(*t*-EDOT-Th) is lower than P(*t*-EDOT-mPy) [35].

3.4 Spectroelectrochemical properties

Figure 5 shows *in situ* UV-Vis-NIR spectroelectrochemistry of the thin films electrochemically deposited on ITO. The absorbance is utilized as an evidence of the process of electronic transition between oxidation and neutral states [1]. The thickness of P(*t*-EDOT-mPy) thin films was 223 nm (Figure 5(a)). We can observe two absorption bands (374.3 and 618 nm) in the visible region in the neutral state at –0.2 V, giving the green conducting polymers. As the applied potential increased, the absorption bands of the first peak decreased and those of the second peak increased. The polymer films lose electrons to form polarons and bipolarons to produce subbands, which decreases the energy of interband transition so

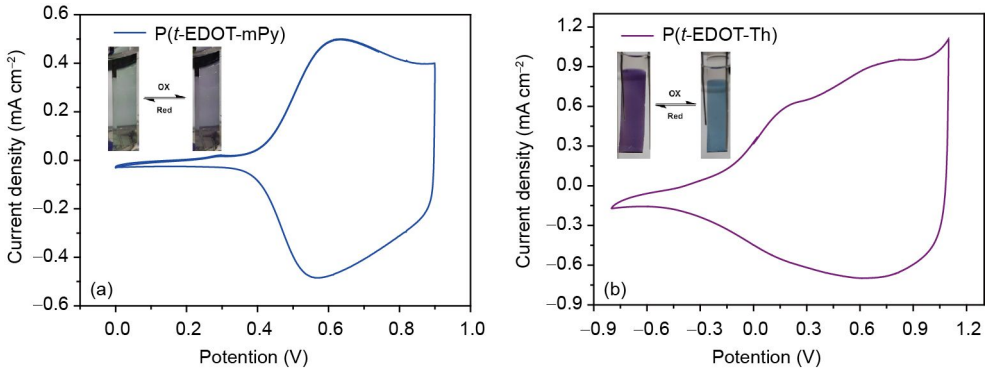

Figure 4 Single cyclic voltammogram and color change of (a) P(*t*-EDOT-mPy) and (b) P(*t*-EDOT-Th) on the Pt electrode (color online).

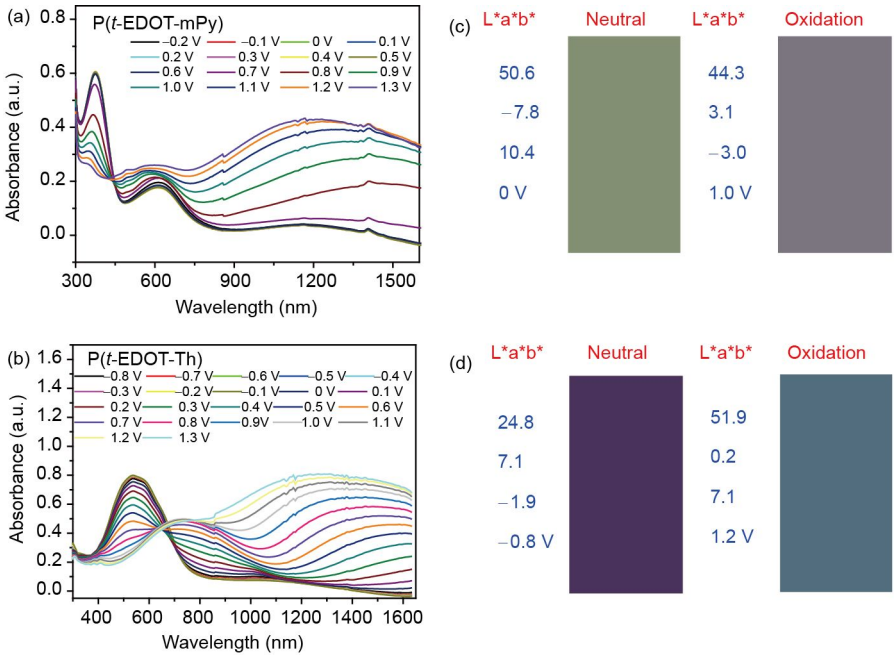

Figure 5 *In-situ* absorption spectra of the polymer films at different potentials. (a) P(*t*-EDOT-mPy) (thickness=223nm) from –0.2 to 1.3 V; (b) P(*t*-EDOT-Th) (thickness=267nm) from –0.8 to 1.3 V. (c, d) CIE of (c) P(*t*-EDOT-mPy) and (d) P(*t*-EDOT-Th) on ITO-coated glass substrate (color online).

that absorption in near infrared region is very high and the polymer has oxidized blue color at 1.3 V. In the reduced state, absorption intensity is weak and similar in the visible region because of totally doped state of the polymer. The band gap is calculated from the onset of the absorption band. From the spectrum, the onset absorption is at 766.8 nm, so the band gap is 1.61 eV for P(*t*-EDOT-mPy), thus we get LUMO=−2.98 eV. Absorption bands of P(*t*-EDOT-Th) are observed in the visible region (Figure 5(b)). The conducting polymer P(*t*-EDOT-Th) gives the neutral-state purple color at –0.8 V with absorption band centered at 535 nm in the visible region. P(*t*-EDOT-Th) gives the oxidation-state dark blue color at 1.3 V. Based on the onset absorption at 732 nm, the band gap is 1.62 eV and the LUMO is –2.54 eV. While, the band gap of poly(BEDOT-T) (1.7 eV) [36], after *bi*-EDOT substitution is lower than PT, here *tetra*-EDOT substitution gives the lowest band gap. The same results are shown by P(*t*-EDOT-mPy). In addition, the absorbance of P(*t*-EDOT-Th) in the oxidation state reaches as high as 80%, while in the reduced state the absorbance is close to zero. Therefore, P(*t*-EDOT-Th) is a promising candidate for application in the infrared camouflage.

The 1976 CIE color coordinates (L*; a*; b*) are used as color space. L* represents luminance, while a* stands for red and green color and b* indicates yellow and blue color [16]. The CIE color coordinate values of two polymers are measured in their neutral and oxidation states respectively. These results are presented in Figure 5(c, d) [10,37]. In the neutral state the (L*; a*; b*) for P(*t*-EDOT-mPy) are (50.6; –7.8; 10.4), giving green zone. Whereas, in the oxidation state, the (L*; a*; b*) are (44.3; 3.1; –3.0), giving purple zone. P(*t*-EDOT-Th), has a purple color in neutral state with corresponding values of (24.8; 7.1; –1.9) and a blue color in oxidation state with corresponding values of (51.9; 0.2; –7.1). In the near infrared region, absorbance difference of P(*t*-EDOT-Th) between oxidized and reduced states is greater than P(*t*-EDOT-mPy).

It is well known that the bandgap of polythiophenes is about 2.2 eV and PEDOTs is about 1.6 eV. The introduction of electron-rich EDOT on thiophene ring can increase its electron density and reduce its bandgap. Therefore, both polymers with four EDOT units have decreased bandgap (1.62 eV for P(*t*-EDOT-mPy) and 1.61 eV for P(*t*-EDOT-Th)). This phenomenon demonstrated that EDOT units play a leading role in the regulation of bandgaps, which is consistent with our prediction. Effective bandgap tuning can be achieved by introducing different groups and adjusting the proportion of different groups, which is helpful to design suitable electrochromic materials.

3.5 Switching time

In order to further probe the characteristics of the synthesized materials, we combined electrochemical workstation with UV-Vis-NIR spectroelectrochemistry to measure the transmittance of two polymer films. In Figure 6, the potentials are between –0.2 and 1.3 V for (P(*t*-EDOT-mPy) and –0.2–1.1 V for P(*t*-EDOT-Th) with a switching interval of 10 s. The transmittance of the polymer P(*t*-EDOT-mPy) is 65.06% in the oxidation state and 56.98% in the neutral state, thus the optical contrast is 8.08% at 370 nm. Under the same condition, the optical contrast is 8.36% at 1500 nm. For P(*t*-EDOT-Th), the optical contrast is 32.7% at 530 nm and 54.3% at 1500 nm. P(*t*-EDOT-Th) shows higher optical contrast because of the obvious color change [38].

3.6 Cycle life

Cycle life is one of the most important indices for assessing the application of electrochromic materials. Repeated cycles of CV reflect the stability of polymer films, because it can result in physical changes. To investigate the stability of polymers, the polymer films on Pt electrode were CV scanned repeatedly for 1000 times from 0 to 0.9 V for P(*t*-EDOT-mPy) and from –0.2 to 0.9 V for P(*t*-EDOT-Th) in the air at a scan rate of 200 mV s^{-1} (Figure 7(a)). The P(*t*-EDOT-mPy) films show 91.8% redox stability after 500 cycles and 86.3% after 1000 cycles. Similarly, the electroactivity of the P(*t*-EDOT-Th) films remained 84.9% after 500 cycles, while it remained 84.5% after 1000 cycles with only 0.4% decrease within corresponding 500 cycles (Figure 7(b)). In spite of more stability of P(*t*-EDOT-mPy) during the first several cycles, the films of P(*t*-EDOT-Th) became more stable than the films of P(*t*-EDOT-mPy) with the increase of cycles.

Switching studies were performed to monitor the optical contrast as a function of time (Figure 8), using double step chronoamperometry method with a switching interval of 10 s for both the films. The average oxidation time of P(*t*-EDOT-mPy) is 1.85 s and the average reduction time is 0.73 s; P(*t*-EDOT-Th) is more quick than P(*t*-EDOT-mPy), the average time of oxidation process is 1.25 s and the reduction process time is 0.95 s, so oxidation process is the rate-determining step (Figure 8).

The coloration efficiency (CE) reflects the electrical energy consumption to change the color. The higher the CE value, the smaller the amount of electricity used in the color change. The CE of P(*t*-EDOT-mPy) at 370 nm and 1500 nm is 44.1 and 90.9 cm^2 C^{-1}, respectively. Whereas P(*t*-EDOT-Th) has CE values of 180.0 and 239.7 cm^2 C^{-1} at 530 and 1500 nm, respectively. Which shows that the P(*t*-EDOT-Th) has higher CE [39,40].

3.7 Morphological studies

In order to observe the surface morphology of the two polymers, AFM imagesi withi 550 nm×550 nm are shown in

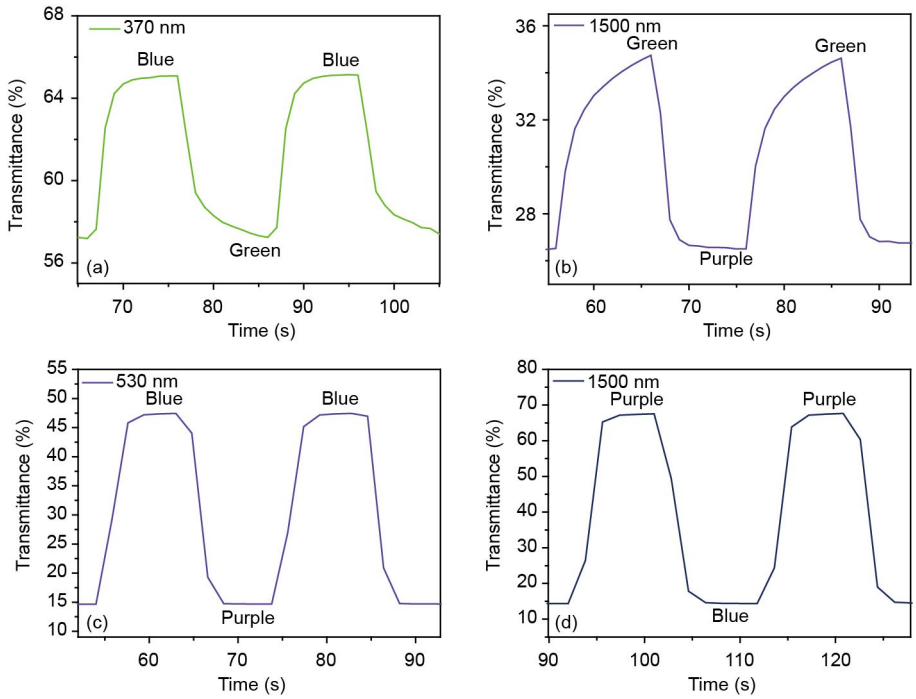

Figure 6 Transmittance changes of P(*t*-EDOT-mPy) at (a) 370 nm, (b) 1500 nm; transmittance changes of P(*t*-EDOT-Th) at (c) 530 nm, (d) 1500 nm (color online).

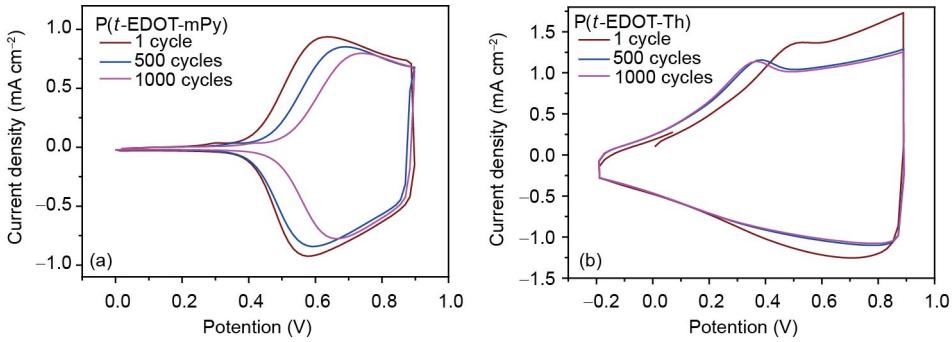

Figure 7 Cycles life of (a) P(*t*-EDOT-mPy) (from 0 to 0.9 V), (b) P(*t*-EDOT-Th) (from –0.2 to 0.9 V) at the scan rate of 200 mV s^{-1} (1 cycle, 500 cycles, 1000 cycles) (color online).

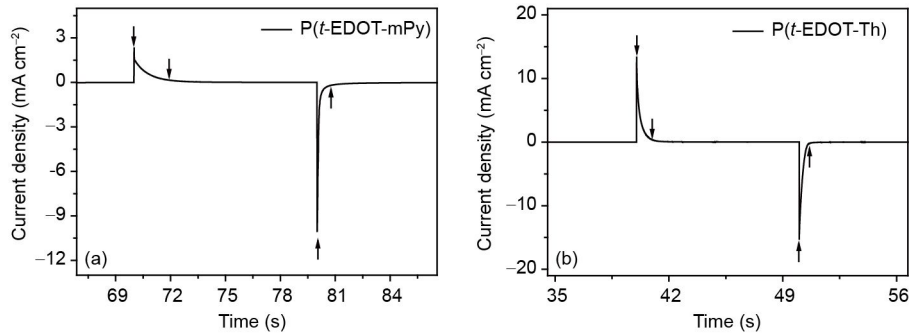

Figure 8 Chronoamperometry of (a) P(*t*-EDOT-mPy) from –0.2 to 1.3 V, and (b) P(*t*-EDOT-Th) from –0.8 to 1.3 V.

Figure 9. Obviously, the two polymers have 3D structures. P(*t*-EDOT-mPy) has a compact surface and the morphology of P(*t*-EDOT-mPy) has a sphere like condensed structure. Whereas, for P(*t*-EDOT-Th), we can clearly observe the agglomeration of particles in Figure 8 which indicates non-covalent interactions between polymer particles.

3.8 Device structure

A sandwich structure could be employed to fabricate OEC devices [4,41]. Polymer films were prepared on an ITO-coated glass by electrochemical polymerization process. After rinsing in a monomer-free electrolyte solution, the films were covered with a gel electrolyte ($LiClO_4$:PVP (M_W=1300000):ACN:PC=3:7:70:20, wt%; PVP=polyvinyl pyrrolidone) and sandwiched with another blank ITO-coated glass (Figure 10) [42]. The device was then allowed to dry by electric hair dryer in air to fix it properly. With a voltage between –2.0 and +2.4 V, both devices have obvious color changes, but polymer P(*t*-EDOT-Th) has more obvious color changes and better device performance.

4 Conclusions

Two novel 3D electrochromic materials are designed and synthesized via multi-position polymerization based on *tetra*-EDOT substitution. The *tetra*-EDOT substituted P(*t*-EDOT-mPy) and P(*t*-EDOT-Th) present 3D structures with reduced band gaps and well-defined redox processes could be observed. The results illustrate that P(*t*-EDOT-Th) possesses shorter color switching rates, higher stability and better performance in the OEC devices as compared to P(*t*-EDOT-mPy). These phenomena are attributed to the characteristics of the functional group and their characteristic band gap plays a vital role in the designing of electrochromic materials. Due to the admirable properties of the two materials, we plan to do further research and explore their properties for their possible incorporation in organic electronics devices, their use as hole injection materials and further enhancement of the optoelectronic properties by replacing PEDOT as P(*t*-EDOT-mPy)/PSS (PSS=poly(styrenesulfonate)) or P(*t*-EDOT-Th)/PSS dispersants.

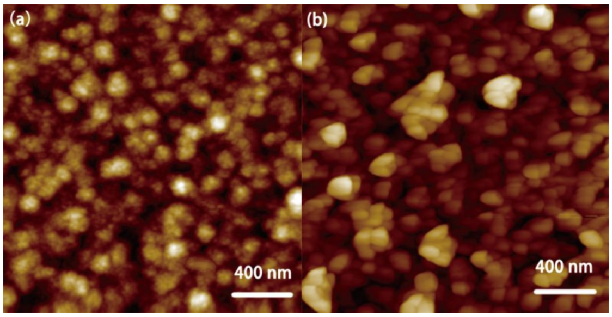

Figure 9 AFM images of (a) P(*t*-EDOT-mPy), (b) P(*t*–ED-OT-Th) at neutral state, respectively (color online).

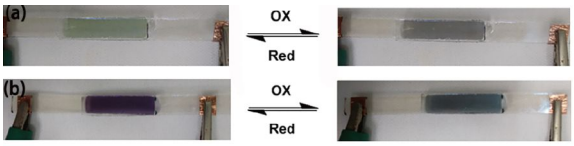

Figure 10 The devices based on (a) P(*t*-EDOT-mPy) and (b) P(*t*-EDOT-Th) (color online).

Acknowledgments This work was supported by the Shenzhen Key Laboratory of Organic Optoelectromagnetic Functional Materials of Shenzhen Science and Technology Plan (ZDSYS20140509094114164), the Shenzhen Peacock Program (KQTD20140627145432 96), Shenzhen Science and Technology Research Grant (JCYJ20140509093817690), the Nanshan Innovation Agency Grant (KC2015ZDYF0016A), the Guangdong Key Research Project (2014B090914003, 2015B090914002), the Guangdong Talents Project, the National Basic Research Program of China (2015CB856505), the National Natural Science Foundation of China (51373075), the Guangdong Academician Workstation (2013B090400016), and the Natural Science Foundation of Guangdong Province (2014A030313800).

Conflict of interest The authors declare that they have no conflict of interest.

1 Mortimer RJ. *Annu Rev Mater Res*, 2011, 41: 241–268
2 Remmele J, Shen DE, Mustonen T, Fruehauf N. *ACS Appl Mater Interfaces*, 2015, 7: 12001–12008
3 (a) Yeh MH, Lin L, Yang PK, Wang ZL. *ACS Nano*, 2015, 9: 4757–4765; (b) Wang Y, Runnerstrom EL, Milliron DJ. *Annu Rev Chem Biomol Eng*, 2016, 7: 283–304
4 Mortimer RJ, Dyer AL, Reynolds JR. *Displays*, 2006, 27: 2–18
5 Yu H, Shao S, Yan L, Meng H, He Y, Yao C, Xu P, Zhang X, Hu W, Huang W. *J Mater Chem C*, 2016, 4: 2269–2273
6 Lehtimäki S, Suominen M, Damlin P, Tuukkanen S, Kvarnström C, Lupo D. *ACS Appl Mater Interfaces*, 2015, 7: 22137–22147
7 Sonmez G, Meng H, Wudl F. *Chem Mater*, 2004, 16: 574–580
8 Wang C, Gu P, Hu B, Zhang Q. *J Mater Chem C*, 2015, 3: 10055–10065
9 Jensen J, Hösel M, Dyer AL, Krebs FC. *Adv Funct Mater*, 2015, 25: 2073–2090
10 Beaujuge PM, Reynolds JR. *Chem Rev*, 2010, 110: 268–320
11 Tagmouti S, Outzourhit A, Oueriagli A, Khaidar M, Elyacoubi M, Evrard R, Ameziane EL. *Sol Energ Mat Sol C*, 2002, 71: 9–18
12 Lin R, Stokbro K, Madsen DN, Boubour E, Bøggild P. *Thin Solid Films*, 2005, 484: 334–340
13 Roncali J, Blanchard P, Frère P. *J Mater Chem*, 2005, 15: 1589–1610
14 Huang JH, Hsu CY, Hu CW, Chu CW, Ho KC. *ACS Appl Mater Interfaces*, 2010, 2: 351–359
15 Agrawal V, Shahjad V, Bhardwaj D, Bhargav R, Sharma GD, Bhardwaj RK, Patra A, Chand S. *Electrochim Acta*, 2016, 192: 52–60
16 Shi J, Zhu X, Xu P, Zhu M, Guo Y, He Y, Hu Z, Murtaza I, Yu H, Yan L, Goto O, Meng H. *Macromol Rapid Commun*, 2016, 37: 1344–1351
17 Taerum T, Lukoyanova O, Wylie RG, Perepichka DF. *Org Lett*, 2009, 11: 3230–3233
18 Xu C, Zhao J, Cui C, Wang M, Kong Y, Zhang X. *J Electroanal Chem*, 2012, 682: 29–36
19 Piron F, Leriche P, Mabon G, Grosu I, Roncali J. *Electrochem Commun*, 2008, 10: 1427–1430
20 Zhong YP, Gao JM, Liu P, Deng WJ. *Mater Res Innov*, 2015, 19: 51–54
21 Zhang K, Tieke B, Forgie JC, Vilela F, Parkinson JA, Skabara PJ. *Polymer*, 2010, 51: 6107–6114
22 Vilela F, Zhang K, Antonietti M. *Energ Environ Sci*, 2012, 5:

7819–7832
23 Liu Y, Kanhere PD, Ling Wong C, Tian Y, Feng Y, Boey F, Wu T, Chen H, White TJ, Chen Z, Zhang Q. *J Solid State Chem*, 2010, 183: 2644–2649
24 Gilow HM, Burton DE. *J Org Chem*, 1981, 46: 2221–2225
25 Sadekar AG, Mohite D, Mulik S, Chandrasekaran N, Sotiriou-Leventis C, Leventis N. *J Mater Chem*, 2012, 22: 100–108
26 Meng H, Perepichka DF, Wudl F. *Angew Chem Int Ed*, 2003, 42: 658–661
27 Sotzing GA, Reddinger JL, Katritzky AR, Soloducho J, Musgrave R, Reynolds JR, Steel PJ. *Chem Mater*, 1997, 9: 1578–1587
28 Li Y. *J Electroanal Chem*, 1997, 433: 181–186
29 Poverenov E, Li M, Bitler A, Bendikov M. *Chem Mater*, 2010, 22: 4019–4025
30 Evans DH. *Chem Rev*, 1990, 90: 739–751
31 Roncali J. *Chem Rev*, 1992, 92: 711–738
32 Andrieux CP, Audebert P, Hapiot P, Saveant JM. *J Am Chem Soc*, 1990, 112: 2439–2440
33 Kumar A, Welsh DM, Morvant MC, Piroux F, Abboud KA, Reynolds JR. *Chem Mater*, 1998, 10: 896–902
34 San Miguel L, Porter WW, Matzger AJ. *Org Lett*, 2007, 9: 1005–1008
35 Durmus A, Gunbas GE, Toppare L. *Chem Mater*, 2007, 19: 6247–6251
36 Sotzing GA, Reddinger JL, Reynolds JR, Steel PJ. *Synth Met*, 1997, 84: 199–201
37 Ak M, Ak MS, Kurtay G, Güllü M, Toppare L. *Solid State Sci*, 2010, 12: 1199–1204
38 Li M, Wei Y, Zheng J, Zhu D, Xu C. *Org Electron*, 2014, 15: 428–434
39 Kim HN, Cho SM, Ah CS, Song J, Ryu H, Kim YH, Kim TY. *Mater Res Bull*, 2016, 82: 16–21
40 Kim H, Park Y, Choi D, Ahn SH, Lee CS. *Appl Surface Sci*, 2016, 377: 370–375
41 Knott EP, Craig MR, Liu DY, Babiarz JE, Dyer AL, Reynolds JR. *J Mater Chem*, 2012, 22: 4953–4962
42 Guan S, Elmezayyen AS, Zhang F, Zheng J, Xu C. *J Mater Chem C*, 2016, 4: 4584–4591